Advances in Geo-Energy Research

Vol. 12, No. 1, p. 52-65, 2024

Original article

Experimental study on dual benefits of improvement of CO_2 enhanced oil recovery and its storage capacity for depleted carbonate oil reservoirs

Xianmin Zhou[1]*, Wei Yu[1], Gang Lei[2], Sarmad Zafar Khan[1], Ridha Al-Abdrabainabi[1], Muhammad Shahzad Kamal[1], Yu-Shu Wu[3]

[1]*Center for Integrative Petroleum Research, College of Petroleum and Geosciences, King Fahd University of Petroleum & Minerals, Dhahran 31261, Saudi Arabia*

[2]*National Center for International Research on Deep Earth Drilling and Resource Development, Faculty of Engineering, China University of Geosciences, Wuhan 430074, P. R. China*

[3]*Department of Petroleum Engineering, Colorado School of Mines, Golden 80401, USA*

Keywords:
Sc-CO_2-EOR
CO_2 storage
reservoir heterogeneity
miscible injection
injectivity
permeability loss

Cited as:
Zhou, X., Yu, W., Lei, G., Khan, S. Z., Al-Abdrabainabi, R., Kamal, M. S., Wu, Y. -S. Experimental study on dual benefits of improvement of CO_2 enhanced oil recovery and its storage capacity for depleted carbonate oil reservoirs. Advances in Geo-Energy Research, 2024, 12(1): 52-65.
https://doi.org/10.46690/ager.2024.04.05

Abstract:
The utilization of supercritical CO_2 in oil and gas reservoir engineering, particularly for enhanced oil recovery, has garnered considerable attention due to its potential to boost hydrocarbon production while reducing CO_2 emissions. This study investigates the improvements achievable in CO_2-enhanced oil recovery and subsequent carbon storage capacity within heterogeneous carbonate reservoirs through supercritical CO_2 miscible injection after seawater flooding. Utilizing a dual-core flooding setup with carbonate core samples exhibiting significant permeability contrast, experiments were conducted under reservoir conditions using live oil, seawater, and supercritical CO_2 miscible injection. To enhance CO_2-enhanced oil recovery and storage within low-permeability zones, a thermal foam gel system was introduced into a highly permeable core after initial supercritical CO_2 miscible injection, effectively sealing off high-permeability zones and improving displacement and storage capacity. Results demonstrate that reservoir heterogeneity notably influences supercritical CO_2-enhanced oil recovery efficiency and sequestration in low permeable regions, with bypass flow in high- permeable regions hindering displacement efficiency and CO_2 storage capacity. However, plugging high-permeability zones using a thermal foam gel system after the initial supercritical CO_2 miscible injection, about 15% extra oil recovery of the pore volume from low-permeability zones was recovered during the second supercritical CO_2 miscible injection, and the equivalent pore space provides a site for storing CO_2 also. Additionally, dynamic characteristic parameters such as injectivity, permeability loss, and endpoint relative permeability related to supercritical CO_2 storage are discussed in this study. The study's outcomes contribute to advancing the understanding of CO_2-enhanced oil recovery and sequestration, facilitating the development of more effective and sustainable reservoir management practices.

1. Introduction

Supercritical CO_2 (sc-CO_2) has widely been widely adopted as a mature technology for enhanced oil recovery (EOR) as a secondary and tertiary oil recovery method in the practice of oilfield development (Kokal and Al-Kaabi, 2010; IEA, 2018). sc-CO_2-enhanced oil recovery (sc-CO_2-EOR) technology includes several methods, including immiscible and miscible displacement and water-alternate-gas (WAG), huff-and-puff, and tapered water-alternate-gas and is also widely applied to increase oil recovery after water flooding for sandstone and carbonate reservoirs (Steinsbø et al., 2014; Al-Otaibi et al., 2018; Kalra et al., 2018). Researchers have

Yandy Scientific Press

*Corresponding author.
E-mail address: j.Zhou53@yahoo.com (X. Zhou); wei.yu@kfupm.edu.sa (W. Yu); leigang@cug.edu.cn (G. Lei); sarmad@kfupm.edu.sa (S. Z. Khan); ridhaa@kfupm.edu.sa (R. Al-Abdrabainabi); shahzadmalik@kfupm.edu.sa (M. S. kamal).

Received February 9, 2024; revised February 27, 2024; accepted March 19, 2024; available online March 22, 2024.

proved that CO_2 immiscible and miscible injection can recover more than 10% to 20% of the original oil in place after water flooding (Enick et al., 2012; Al-Otaibi et al., 2018), which is due to the capability of CO_2 to dissolve in the reservoir oil, and thus results in reducing the oil viscosity, oil swelling and extraction of light components of crude oil (Enick et al., 2012). Approximately 100 projects of CO_2 displacements in different oilfields worldwide were reported by The International Energy Agency (IEA, 2019), but studies on the use of depleted oil reservoirs as a storage site for CO_2 have only been carried out in the last decade or so. Additionally, the sequestration of sc-CO_2 has garnered significant attention as a promising technique for optimizing hydrocarbon production and mitigating greenhouse gas emissions (Bachu, 2000; Zhang et al., 2023).

Scientists have focused on the fact that depleted oil reservoirs as CO_2 storage sites are based on the following advantages:

1) Equipment used on the surface and in the injection and production wells can be utilized for CO_2 storage projects after the CO_2-EOR process (Hannis et al., 2017; Cao et al., 2020);
2) During field exploration and production processes, a comprehensive characterization of static and dynamic parameters was conducted. These include properties of the formation and caprock, residual phases (water and oil), and maximum CO_2 saturation. (Orlic, 2016; Cao et al., 2020);
3) The reservoir environmental requirements for CO_2 storage sites are similar to those for oil reservoirs under pore pressure and overburden pressure caused by overlying formation (Carroll et al., 2014; Orlic, 2016; Cao et al., 2020);
4) Because of the prolonged interaction between liquid phases (water and oil)/mineral/CO_2 during the CO_2-EOR injection process, some dynamic parameters such as injectivity and relative permeability of CO_2 tend to be stable, which favors injecting CO_2 only into the formation for the CO_2 storage (Zhou et al., 2023).

However, the effectiveness of CO_2-enhanced oil recovery and CO_2 storage in depleted oil reservoirs can be influenced by various factors, including the geological properties of depleted oil reservoirs (Ennis-King and Paterson, 2002; Zhang et al., 2022). Reservoir heterogeneity is a major factor influencing the oil recovery at the breakthrough and final oil recovery and has been investigated physically in the laboratory and through numerical simulation (Khosravi et al., 2014; Ampomah et al., 2016; Alfarge et al., 2017; Al-Bayati et al., 2018; Hadipoor et al., 2020), and plays a critical role in determining oil recovery through CO_2 injection and the storage capacity of the reservoir (Imanovs et al., 2020).

In laboratory experiments of the CO_2-enhanced oil recovery process, researchers examined how permeability variability impacts oil recovery through the CO_2 miscible displacement process. They reported that CO_2-EOR depends on the level of heterogeneity and permeability contact (Ding et al., 2017). Due to the bypass effect of the high permeability zone, a large volume of oil is trapped in the low permeable formation because of CO_2 bypassing the high permeable zone, thereby resulting in higher oil production in homogeneous cores than in heterogeneous cores (Ding et al., 2017). Investigations on hydrocarbon recovery through CO_2 miscible injection in heterogeneous cores with fractures have revealed that the permeability of fractures plays a crucial role in controlling CO_2 displacement efficiency. These studies have reported 30% to 90% of oil recovery due to this phenomenon (Khosravi et al., 2014; Fernø et al., 2015). The effect of injecting patterns on the recovery of hydrocarbons by soaking and WAG processes and reported that the improved oil recovery is related to injection patterns (Li and Gu, 2014; Sæle et al., 2022). Sæle et al. (2022) investigated the CO_2 foam generated by the surfactant-alternating-gas process to increase oil recovery and associated CO_2 storage capacity. The results show that more oil was recovered, and CO_2 storage capacity was increased compared to CO_2 injection only and the WAG process. In a recent experimental work by Hadipoor et al. (2020), the effect of reservoir heterogeneity and injection pattern on the effectiveness of the CO_2 miscible and immiscible displacements was investigated using cores with varying permeability levels. The findings demonstrate that even a slight permeability alteration can significantly affect miscible and immiscible displacement processes. Moreover, the study reveals that employing a multi-contact-miscible injection process can yield high oil recovery (Hadipoor et al., 2020). Regarding the numerical simulation of CO_2-EOR, previous literature (Ettehadtavakkol et al., 2014; Ampomah et al., 2016) has provided valuable insights into the numerical simulation of CO_2-EOR. These works have presented a comprehensive design framework for CO_2-EOR and storage, specifically focusing on characterizing CO_2 properties and optimizing CO_2 injection strategies using numerical models. Luo et al. (2022) carried out a numerical investigation using the TOUGH2MP-TMVOC model to study the effect of reservoir heterogeneity, specifically porosity, and permeability, on CO_2-EOR, storage capacity, and flow behavior in low permeable oil reservoirs. In addition, they investigated the influence of two key parameters, natural fracture intensity and oil pathway conductivity, on the effectiveness of the carbon dioxide huff-n-puff technique in shale formations. Modeling results indicated that higher natural fracture intensity positively affected oil displacement efficiency, whereas greater oil pathway conductivity had a negative impact. Additionally, the research found that properties of natural fractures, such as porosity and permeability, changed over production time, unlike the molecular diffusion-driven CO_2-EOR process seen in field shale oil reservoirs. CO_2 storage sites in oil or gas reservoirs can be categorized into depleted oil reservoirs, depleted gas reservoirs, operational oil reservoirs, and saline aquifers (Korbøl and Kaddour, 1995; Sengul, 2006; Wei et al., 2023; Zhou et al., 2023). The primary mechanisms contributing to the CO_2 storage capacity in operational or depleted oil formations are as follows: Structural and stratigraphic trapping of gaseous CO_2 and sc-CO_2, solubility trapping in the formation water or remaining water after waterflooding and residual oil, and mineral trapping (Shaw and Bachu, 2002; Shen et al., 2009; Sun and Chen, 2012; Ding et al., 2019; AlRassas et al., 2021). For an oil reservoir serving as a CO_2

Table 1. Composition of formation brine and seawater.

Salt	Formation brine (g/L)	Seawater (g/L)
NaCl	150.446	41.041
$CaCl_2 \cdot 2H_2O$	69.841	2.384
$MgCl_2 \cdot 6H_2O$	20.396	17.645
Na_2SO_4	0.518	6.343
$NaHCO_3$	0.487	0.165
Total dissolved solids	213,734	57,670

Table 2. Physical properties of fluids.

Liquid	Ambient conditions		Reservoir conditions	
	Density (g/cc)	Viscosity (cP)	Density (g/cc)	Viscosity (cP)
Formation water	1.1462	1.45	1.0906	0.73
Seawater	1.0385	0.97	1.0018	0.5
Dead crude oil	0.881	20.51	0.823	2.5
Live oil	/	/	0.755	0.73
Sc-CO_2	/	/	0.5337	0.04

storage site, two distinct scenarios need to be considered: one involves a reservoir where oil is naturally produced, with a significant amount of oil remaining in the formation, and the other pertains to a depleted oil reservoir that has undergone CO_2-EOR processes. Comparatively, when comparing an oil reservoir to a saline aquifer as a CO_2 storage site, the oil reservoir contains a substantial amount of oil within its pore space, while the depleted oil reservoir predominantly contains remaining oil and residual water, in addition to the formation water and bottom water (Shaw and Bachu, 2002; Shen et al., 2009). Zhou et al. (2023) reported that when water flooding is employed as the secondary production technique, followed by CO_2 injection as a tertiary method, some volumes of fluids, such as seawater and residual oil, occupy in the pore space of the formation.

When planning the implementation of CO_2-EOR and estimating CO_2 storage capacity, two crucial factors must be considered concurrently: the CO_2 displacement efficiency and the CO_2 storage factor, which represents the proportion of the amount of CO_2 stored to the amount of CO_2 injected (Shen et al., 2009; Yue et al., 2022) have evaluated the CO_2 storage capacity at breakthrough and any hydrocarbon pore volume injection for oil reservoirs. Ding et al. (2019) proposed expressions to determine the storage capacity of CO_2 dissolved in remaining oil and residual water in depleted oil reservoirs, in addition to providing an empirical expression to estimate the CO_2 storage capacity in oil formations. Moreover, Ding et al. (2022) discussed oil formations' CO_2 usage and storage coefficients. The CO_2 storage capacity resulting from mineral trapping, which involves the reaction between salt water, CO_2, and rocks, is often neglected due to the slow reaction rate and the time required for significant mineralization, typically considered within the first 20 years to account for storage capacity (Ding et al., 2017). As obtaining quantitative measurements of CO_2 storage resulting from mineral trapping is extremely challenging experimentally, modeling techniques have been developed to estimate storage capacity in CO_2/salt water/rock systems (Ding et al., 2017).

This paper presents a practical experimental work that aims to study the impact of reservoir heterogeneity on sc-CO_2-EOR and sequestration in depleted carbonate oil reservoirs, how to improve CO_2 storage capacity and utilization efficiency of the pore space, and evaluate sc-CO_2 storage capacity in the core scale. To simulate the reservoir heterogeneity, a dual-core flooding experiment system was utilized, consisting of two reservoir carbonate core samples with varying permeabilities and porosities. The experimental sequences involve preparation, seawater flooding, and initial and second sc-CO_2 miscible injection at conditions representing the reservoirs. To address the challenges posed by reservoir heterogeneity and recover the residual oil in the low permeable zone, a thermal foam gel slug (TFGS) system is implemented as a conformance control technology in the zone of high permeability. This approach aims to enhance the productivity of sc-CO_2 displacement and enhance oil recovery and CO_2 storage capacity. Furthermore, this study explores various dynamic characteristic parameters such as injectivity and permeability loss to evaluate the injection pattern and assess the CO_2 storage potential in practical field applications. These parameters furnish a deeper understanding of the behavior of sc-CO_2 during the EOR and sequestration processes.

2. Experiments

2.1 Fluids

This study used two types of brins for different purposes: formation water, seawater, crude oils (dead and live crude oils), and sc-CO_2.

Brines: Two brines, formation water and seawater, were utilized for different experiments. Formation water was used to establish the irreversible water saturation (S_{wi}) of the testing core plug. Seawater was utilized as a displacing agent for the water flooding experiment, which can evaluate secondary oil recovery by water flooding (AlOtaibi et al., 2016). The components and properties of the formation water and seawater are listed in Tables 1 and 2, respectively.

Dead and live crude oils: This study used two crude oils (dead oil and live oil). The dead crude oil sample was from a carbonate oil reservoir and was used to establish the irreversible water saturation (S_{wi}) in the core plug and restore the reservoir wettability by the core flooding method. Live crude oil as a displaced phase was used for the experiments on secondary and tertiary oil recovery processes. According to the gas and oil ratio, the live crude oil was combined with dead oil and natural gas. The properties of dead crude oil and live oil at ambient and reservoir conditions are listed in Table 2.

Sc-CO_2: We purchased the sc-CO_2 with a purity of 99.99%

Table 3. Routine core properties.

Core	Sample #	Length (cm)	Diameter (cm)	Kair (mD)	Porosity (frc.)	Pore volume (cc)	Brine permeability (mD)
	A	3.03	3.8	917.3	0.281	9.5	
1D	B	3.36	3.8	746	0.291	11.06	750
	Total	6.39	3.8	831.7	0.286	20.56	
	C	2.88	3.8	51.5	0.194	6.25	
10D	D	3.14	3.8	86.5	0.243	7.84	22.3
	Total	6.02	3.8	69	0.219	14.09	

from a local store. It is used as a displacing agent for enhanced oil recovery by water flooding and the sc-CO_2 miscible injection at reservoir conditions: A pore pressure of 3,200 psi, confining pressure of 4,500 psi, and temperature of 102 °C). The miscible phase with live crude oil in the formation is created under such conditions. During the experiment, the injection pressure was much higher than the minimum miscibility pressure to ensure a miscible phase was formed in the reservoir. The viscosities and densities of the sc-CO_2 at the reservoir conditions are listed in Table 2 as well.

2.2 Core preparation

In this study, we chose four core samples (Core plug ID: A, B, C, and D) from the same carbonate reservoir formation, where the oil and natural gas were taken. Before experimenting to measure the core samples' porosity, pore volume, and brine permeability, we cleaned them using methanol and toluene through the distillation extraction method. Subsequently, we dried the selected core plugs in an oven at 104 °C until their dry weight remained constant. The composite core, 1D, consists of two core plugs, as shown in Table 3, representing the highly permeable core plugs (HPCP) of 832 mD. On the other hand, the composite core, 10D, includes two core plugs, as shown in Table 3, which represent low-permeability core plugs (LPCP) of 69 mD. Table 3 provides a detailed overview of the information on the individual cores and composite core plugs.

2.3 Dual-core flooding apparatus

We designed a custom dual-core flooding apparatus in-house for conducting water flooding and sc-CO_2 miscible injection experiments under reservoir conditions. The aim was to investigate how reservoir heterogeneity affects oil recovery and sc-CO_2 storage capacity. The apparatus comprised two core holders, each holding a core plug with different permeabilities and porosities (HPCP and LPCP). The core holders were positioned horizontally, with the HPCP core holder placed on top of the LPCP core holder to simulate horizontal displacement. A confining pump was employed to control the confining pressure for both core holders to ensure consistent confining pressure conditions. For the injection process, an injection pump connected with several accumulators to load seawater, TFGS, and sc-CO_2 was utilized, enabling the injection of fluids either separately or simultaneously into the two core holders. In this study, we used one pump to inject seawater or sc-CO_2 into both LPCP and HPCP simultaneously. The pore pressure could be adjusted individually or simultaneously using back pressure regulators. A comprehensive data acquisition system was implemented to capture relevant data. It automatically recorded injection flow, testing temperature, upstream and downstream pressure, differential pressure, and pore pressure during seawater flooding, TFGS injection, and sc-CO_2 miscible injection. A visual reference, Fig. 1, illustrates the flow chart of the dual-core flooding apparatus.

2.4 Preparation of seawater flooding and sc-CO_2 miscible injection

Several steps were undertaken to prepare for seawater flooding, thermal foam gel system injection, and sc-CO_2 miscible injections. These included saturating the core plug with formation water, desaturating the core using both dead and live crude oil to establish S_{wi} and establishing original oil in place (OOIP) or original oil saturation (S_{oi}), and aging the composite rock with dead oil and live oil to restore the reservoir wettability of the core sample.

Initial water saturation: To establish the S_{wi}, the dry core plugs were first subjected to 24 hours of vacuum using a vacuum pump. Subsequently, the plugs were saturated with formation water, and the weight change before and after the saturating of the sample was used to determine the pore volume and effective porosity of the core. The saturated core plugs were then immersed in formation water for approximately ten days to achieve ionic equilibrium on the surface of the pore space of the core samples. This process resulted in aged core plugs with formation water. Next, the aged formation water was displaced with fresh formation water about approximately ten pore volumes. In this step, the brine permeability of the core plug was measured at ambient conditions. Following this, the experiments to establish the S_{wi} and S_{oi} were conducted by oil flooding on the core plugs, which were flooded with fresh formation water.

Process of assembly composite core: Upon completing the aging process of the individual core samples with formation water, core plugs A and B were combined to create a high permeability core plug labeled as composite core, 1D. Similarly, the composite core, 10D comprising core samples C

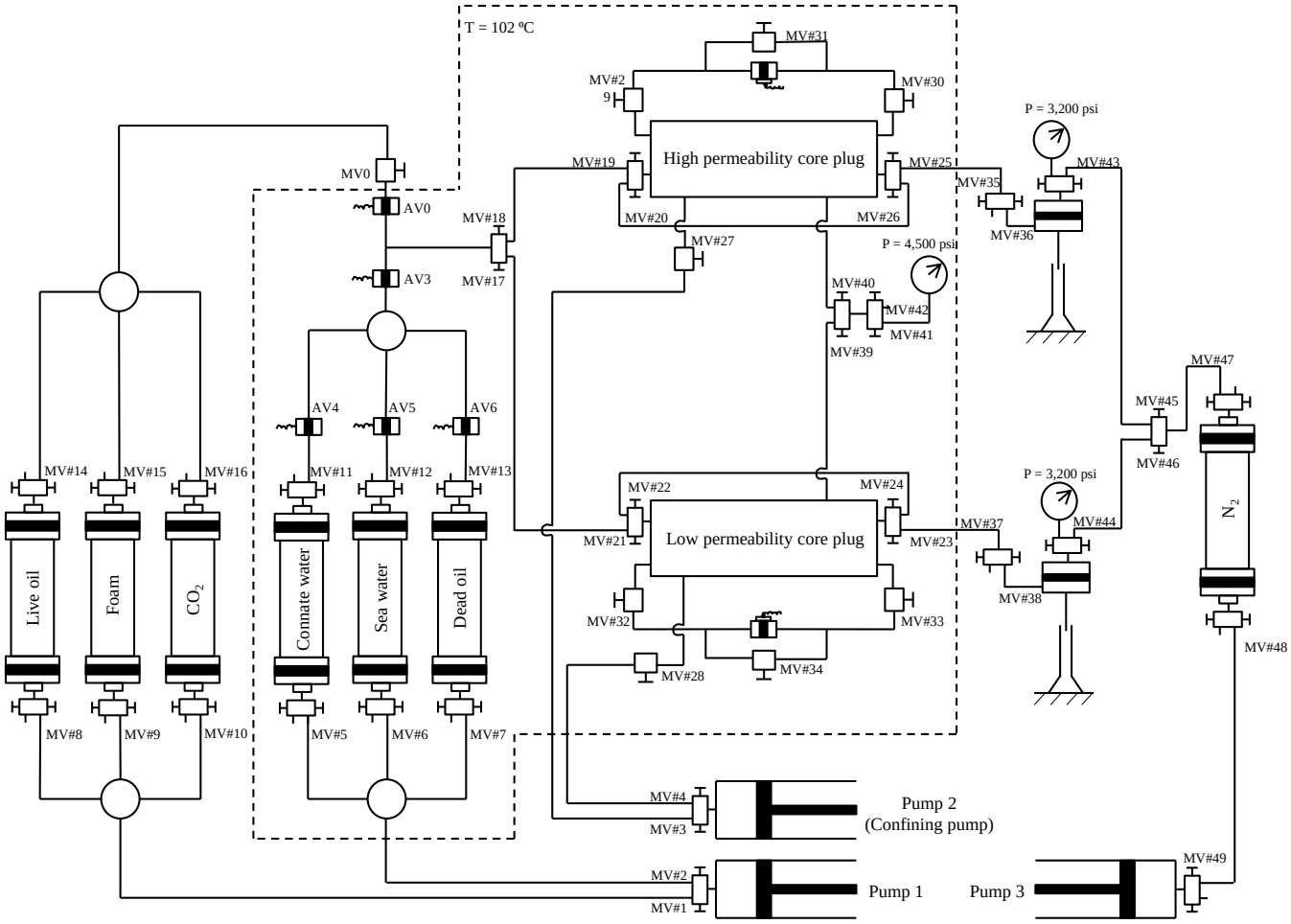

Fig. 1. The flow chart of the dual-core flooding apparatus.

and D, represents the low permeable zone. The procedure for assembling a composite core is as follows:

1) The individual core plugs A and B were brought into contact and secured using Teflon tape, forming an assembled composite core.
2) To prevent the diffusion of sc-CO_2 between the composite core and the rubber sleeve, a layer of aluminum foil was applied to the Teflon tape.
3) The assembled composite core, Teflon tape, and aluminum foil were inserted inside a heat shrink tube and subjected to heat using a heating gun. This process ensured a firm bond, creating an integrated composite core sample.

2.5 Aging core with two types of oil

Following proccess of assembly of composite core, the experiments to establish the S_{wi} and S_{oi} were performed on the testing core saturated with fresh formation water.

Dead crude oil flooding: We loaded the composite core saturated fully with fresh formation water into the core holder, and then the water was flooded by dead oil with multiple injection flow rates from 0.1 to 2.0 cc/min at ambient conditions. During the oil flooding of each injection flow rate, the amount of produced formation water from the testing core and the differential pressure between the inlet and outlet of the core was measured and recorded until no water was further produced. To form a uniform distribution of initial water, a reverse flooding process is necessary. At this step, S_{wi} and S_{oi} were determined through the material balance based on the volume of formation water in the core and the amount of produced water during oil flooding, and the effective oil permeability at S_{wi} was also calculated using the Darcy equation.

Live crude oil injection: The purpose of aging core plugs with crude oil and live oil is to restore the wetting behavior of the testing cores to reflect reservoir wettability. After we used dead crude oil to establish the core plugs' initial water and oil saturations, live crude oil flooding was conducted on all testing cores under the testing conditions. During the aging process, the testing core was injected with approximately one pore volume (PV) of live crude oil per day at 1.0 cc/min for three weeks. This step aimed to restore the wettability of the cores under reservoir conditions. Differential pressure measurements were taken across the core plugs during live crude oil injection to assess the stability of the oil and ensure that the composite core remained undamaged throughout the process. After aging the testing cores with dead and live crude

Table 4. Initial conditions of two composite cores before the seawater flooding experiment.

Core	Pore volume (cc)	S_{wi} (% PV)	V_w (cc)	V_o (cc)	S_{oi} (% PV)
1D (HPCP)	20.56	24.6	5.06	15.5	75.4
10D (LPCP)	14.06	17.56	2.47	11.59	82.44

Notes: V_w: Water volume in the core; V_o: Oil in the core; S_{oi}: Original oil saturation.

oil, it was supposed to exhibit weakly oil-wet or mixed-wetting characteristics, as Okasha et al. (2007) stated. Table 4 details the S_{wi} and S_{oi} in the testing cores for such experiments. The orientation of the experiment for water flooding and sc-CO_2 miscible injection processes is horizontal.

2.6 Seawater flooding experiment

The experiment of seawater flooding was conducted to achieve several objective concerns. These objectives included determining oil recovery factors, assessing the productivity of seawater flooding, and establishing the residual oil saturation and maximum water saturation before sc-CO_2 miscible injection. The seawater flooding was carried out under specific conditions described in Section 2.1. Table 4 provides the S_{wi}, S_{oi}, and V_o (OOIP) values for composite cores 1D and 10D. Table 5 outlines the injection flow rate employed during the core flooding experiments in this study.

Seawater was simultaneously injected into composite core 1D (HPCP) and composite core 10D (LPCP) at varying injection flow rates during the experiment. We chose the injection flow rate of 0.5 cc/min for injection pore volume (IPV), 1.0 cc/min for 1 IPV, and 2.0 cc/min for 1 IPV. The seawater flooding is typically completed when the water cut reaches approximately 99%. Throughout the dual-core flooding test, the oil produced from the cores was collected over time and recorded against the volume of seawater injected. The upstream and downstream pressure and the differential pressure across the composite core plug were automatically monitored. It's important to note that the oil production, upstream and downstream pressure, and differential pressure were separately recorded for HPCP and LPCP.

2.7 Initial supercritical carbon dioxide miscible injection

Following the seawater flooding, some residual oil persists in the HPCP and LPCP. This remaining oil becomes the target for the EOR process. To achieve the displacement of this remaining oil, we employed sc-CO_2 as the displacing agent in this study. The objective was to achieve miscible displacement with the remaining oil in both composite cores, thereby enabling additional oil recovery through the sc-CO_2 miscible injection process. The experimental conditions, including pore pressure, confining pressure, and temperature, remained consistent with those of the seawater flooding phase.

Table 5. Injection flow rate for water flooding and sc-CO_2 miscible injection.

Core	Flow rate (cc/min)	
	Water flooding	Sc-CO_2 flooding
1D (HPCP) 10D (LPCP)	0.5, 1.0, 2.0	0.5

The sc-CO_2 was injected simultaneously into the HPCP and LPCP at a constant injection flow rate of 0.5 cc/min. This phase is referred to as the initial sc-CO_2 miscible injection. Various parameters were monitored and recorded during the initial sc-CO_2 miscible injection process for the HPCP and LPCP, respectively. These included oil and water production, upstream and downstream pressure, and differential pressure. These parameters were automatically measured using a data acquisition system to assess the performance of the sc-CO_2 injection process for HPCP and LPCP.

2.8 Injection of thermal foam gel system

To recover the remaining oil left in the LPCP following the initial sc-CO_2 injection, a conformance control technology known as thermal form gel slug (TFGS) was implemented to enhance displacement efficiency, as described by Zhou et al. (2020b). To improve the remaining oil and the sc-CO_2 storage capacity in the LPCP, approximately 0.4 PV of TFGS were flooded into the zone of high permeability at 0.5 cc/min of injection flow rate. The purpose of the TFGS injection was to block the larger pores within the HPCP, and the sc-CO_2 can be displaced into the LPCP, ultimately enhancing the overall efficiency of the process. During the TFGS injection, the LPCP was isolated, and the differential pressure within the HPCP was recorded. This allowed for monitoring and analysis of the pressure changes occurring within the system during the TFGS injection stage.

2.9 Second supercritical carbon dioxide miscible injection

Following the completion of the TFGS injection, the second sc-CO_2 miscible injection was immediately started to recover the remaining oil in the LPCP after the initial sc-CO_2 miscible injection. The injection was carried out at 0.5 cc/min of a constant flow rate. To conduct the second sc-CO_2 miscible injection, the inlet valves for the LPCP and HPCP cores, which controlled the flow of sc-CO_2 into the cores, were opened. This allowed the sc-CO_2 to be injected into both composite cores simultaneously. During the process of the supercritical carbon dioxide miscible injection, various measurements were recorded. These included oil and water production and upstream and downstream pressure. Additionally, the differential pressure within both the LPCP and HPCP was monitored. This comprehensive data collection enabled the monitoring and analysis of pressure changes occurring within the system during the second miscible injection stage.

Table 6. Summary of water flooding and sc-CO_2 injection.

Core	Water flooding			sc-CO_2					
	ORF (% PV)	$S_{w(max)}$ (% PV)	S_{orw} (% PV)	Initial ORF (% PV)	Second ORF (% PV)	Total ORF (% PV)	$S_{sc-CO_2(max)}$ (% PV)	$S_{orsc-CO_2}$ (% PV)	S_{wr} (% PV)
1D	38.41	62.9	37.12	35.7	/	35.7	71.9	1.36	26.74
10D	34.14	51.7	48.29	18.8	15.1	33.9	56.96	14.44	28.6

Notes: ORF: Oil recovery factor; $S_{w(max)}$: Maximum water saturation; S_{orw}: Water-flooded remaining oil saturation; $S_{sc-CO_2(max)}$: Maximum sc-CO_2 saturation; $S_{orsc-CO_2}$: Residual oil saturation at last stage of the supercritical carbon dioxide miscible injection is completed; S_{wr}: Residual water saturation at last stage of the supercritical carbon dioxide miscible injection is completed.

3. Results and discussion

3.1 Oil recovery

Four core flooding experiments were conducted using carbonate cores and live oil under the reservoir conditions to study the oil recovery factors of seawater flooding, sc-CO_2 miscible injection, and evaluate the sc-CO_2 storage potential for depleted carbonate oil reservoirs. These experiments included seawater flooding, initial sc-CO_2 miscible injection, TFGS injection, and second sc-CO_2 miscible injection. In addition, several dynamic characteristic parameters, such as injectivity and endpoint relative permeability, are discussed to evaluate CO_2 storage potential.

3.1.1 Oil recovery by seawater flooding

An experiment in which two cores have different permeability was performed under reservoir conditions to assess the effect of reservoir heterogeneity on oil recovery factors and the storage capacity of sc-CO_2. The initial values, including initial water saturation, pore volume, and water and oil saturations, are detailed in Table 4 before the commencement of the seawater injection experiment. Initially, seawater was simultaneously injected into both composite cores, 1D and 10D, representing the zones of high and low permeability, respectively, at varying flow rates. The injection pattern was a horizontal-continuous injection approach. The experiment was terminated upon getting a water production of 99% of the total flow, indicating the attainment of remaining oil saturations in both the high and low permeable zones. This marked the completion of injecting 4.0 pore volumes of seawater. Table 6 presents the characteristic parameters, such as oil recovery factors and remaining oil saturation, resulting from the seawater injection for both 1D and 10D. These calculations were performed using the material balance method based on the experimental data, including oil and water productions during the seawater injection process, the composite sample's pore volume, and the sample's original oil content. Table 6 reveals that the water-flooded remaining oil saturations were 37.1% PV for 1D and 48.3% PV for 10D, highlighting the influence of rock permeability on the results.

Based on the seawater injection experiment observations, a significant amount of oil remained in both cores, indicating the potential for recovery and storage through sc-CO_2 miscible injection as a tertiary oil production process.

3.1.2 Oil recovery by initial supercritical carbon dioxide miscible injection

To recover the remaining oil left in both the high and low permeable zones, the initial sc-CO_2 miscible injection was injected in tertiary mode. The injection was carried out at a rate of 0.5 cc/min, and the pore pressure and temperature utilized for this experiment were the same as seawater flooding. It's worth noting that the minimum miscibility pressure between live oil and sc-CO_2 under testing conditions was determined to be 2,600 psi, significantly below the pore pressure of 3,200 psi (Al-Otaibi et al., 2018). This ensures the formation of a miscible displacement during the sc-CO_2 injection process. The sc-CO_2 was injected simultaneously into the HPCP and LPCP. Real-time monitoring of oil and water production allowed for the calculation of oil recovery through the initial sc-CO_2 miscible injection and measurement of residual water in the composite cores. The amount of residual water in the cores was utilized to estimate the capacity of sc-CO_2 solubility in residual water (Zhou et al., 2023).

Table 6 provides an overview of oil recoveries achieved through the initial sc-CO_2 miscible injection for HPCP and LPCP. In the case of the HPCP, most of the remaining oil after water flooding was successfully recovered through the initial sc-CO_2 miscible injection, resulting in residual oil content of only 1.4% of the PV. Most of the pore space was occupied by the sc-CO_2, about 72% of PV, which means the higher the oil recovery factor, the greater the sc-CO_2 sequestration potential. However, for the LPCP, an oil recovery of 18.8% of PV was attained through the initial sc-CO_2 miscible injection, leaving approximately 30% of crude oil remaining in the LPCP. Notably, during the initial sc-CO_2 miscible injection, no further oil production was observed from the LPCP following the breakthrough of sc-CO_2 in the HPCP. This suggests that sc-CO_2 did not effectively displace the water-flooded remaining oil in the LPCP. This outcome can be attributed to reservoir heterogeneity or the permeability contrast affecting oil production.

The conformance control technique utilizing the TFGS system was implemented in the HPCP to produce the remaining oil in the LPCP after the initial supercritical carbon dioxide miscible injection.

3.1.3 Evaluation of thermal foam gel injection

To produce the residual 30% of crude oil left behind in the LPCP after initial sc-CO_2 injection and improve sc-CO_2 storage capacity, we proceeded to inject the TFGS system exclusively into the high permeable zone (HPCP) at a constant injection rate of 0.5 cc/min. Approximately 0.4 PV of the TFGS system were injected into the HPCP by closing the inlet valve for the LPCP, effectively plugging the pores within the HPCP. During the TFGS injection process, close monitoring and recording of the upstream and differential pressure across the HPCP were conducted. The injection of the TFGS system was halted when the differential pressure, also known as the blocking pressure, reached 200 psi, and TFGS was injected into the HPCP at about 0.4 PV. Comparing the injection pressure recorded during the initial sc-CO_2 miscible injection in the LPCP (less than 10 psi) with the blocking pressure of 200 psi generated during the TFGS experiment in the HPCP, it can be concluded that the blockage effect was deemed satisfactory (Zhou et al., 2020a). Consequently, the following sc-CO_2 miscible injection process is expected to improve the sweep efficiency due to the successful implementation of the TFGS system, which effectively plugged the pores within the HPCP.

3.1.4 Second supercritical carbon dioxide miscible injection for oil Recovery

In the second supercritical carbon dioxide miscible injection, the HPCP and LPCP were opened to allow for injecting sc-CO_2 into both cores. The flow rate is similar to the initial supercritical carbon dioxide miscible injection process. As a result of the blockage in the high permeability zone, the supercritical carbon dioxide was injected significantly toward the low permeable zone. It observed that the crude oil was produced only from the LPCP, as the HPCP had already reached a residual state. In other words, no oil was recovered from the HPCP during this stage.

The second sc-CO_2 miscible injection yielded a recovery of approximately 15.1% of the pore volume (PV) or 19% of the OOIP for the LPCP, which increases the sc-CO_2 storage capacity because such pore space was occupied with remaining oil after the initial sc-CO_2 miscible injection. Thus, sc-CO_2 saturation reached the maximum value of 57% of the pore volume. The total oil recovery of 33.9% PV was produced during the initial and second sc-CO_2 miscible injection, with approximately 14.4% of the PV representing the residual oil content in the LPCP, as indicated in Table 6. The results show that applying the TFGS system improves displacement efficiency and increases the sequestration capacity of supercritical carbon dioxide in the low permeable zone.

3.2 Supercritical carbon dioxide storage capacity in core scale

The effective utilization of the pore space within the formation is crucial for successful sc-CO_2 geological sequestration in a depleted carbonate oil reservoir. The displacement efficiency achieved through sc-CO_2 miscible injection was directly influenced by pore space utilization, which determines the distribution of the sc-CO_2 saturation, residual oil saturation, and water saturation when the injection process was completed. Evaluating the total sc-CO_2 storage capacity relies primarily on parameters such as sc-CO_2 saturation (structure trapping), residual oil saturation (dissolution trapping of sc-CO_2 in residual oil), and residual water saturation (dissolution trapping of sc-CO_2 in the residual water), which are measured at the laboratory scale (Zhou et al., 2023). It's important to note that the mineral trapping resulting from the interaction between sc-CO_2, seawater, and carbonate rock is negligible in this study, as it may not fully represent the conditions observed in an actual oil field practice (Benson et al., 2012). Considering the sc-CO_2 storage capacity based on the core flooding experiment, an expression can be derived to calculate the total amount of sc-CO_2 storage capacity M_T in a depleted core or oil reservoir:

$$M_T = M_1 + M_2 + M_3 \tag{1}$$

where M_1 represents the sc-CO_2 storage capacity in the pore space previously occupied by recovered water and oil before miscible injection (structure trapping), the calculation for M_1 can be expressed as follows:

$$M_1 = S_{\mathrm{sc-CO_2(max)}} V_p \rho_{\mathrm{sc-CO_2}} \tag{2}$$

where $S_{\mathrm{sc-CO_2(max)}}$ represents the maximum sc-CO_2 saturation, which reached at the end of the sc-CO_2 miscible injection, expressed as a % PV; V_p represents the pore volume of the core.

Parameter M_2 in Eq. (1) represents the sc-CO_2 storage capacity for dissolving sc-CO_2 in residual oil (dissolution trapping), which depends on the residual oil saturation, $S_{or(\mathrm{sc-CO_2(max)})}$, and the dissolution coefficient in the oil phase, $C^o_{\mathrm{sc-CO_2}}$. The calculation for M_2 is as follows:

$$M_2 = S_{or(\mathrm{sc-CO_2(max)})} \rho_{\mathrm{sc-CO_2}} C^o_{\mathrm{sc-CO_2}} V_p \tag{3}$$

where $C^o_{\mathrm{sc-CO_2}}$ corresponds to the dissolution coefficient of sc-CO_2 in the oil phase, which is 0.366 in this study (Zhang et al., 2010).

Parameter M_3 in Eq. (1) represents the sc-CO_2 storage capacity for dissolving sc-CO_2 in residual water. This capacity depends on the residual water saturation, $S_{wr(\mathrm{sc-CO_2(max)})}$, and the dissolution coefficient in the water phase, $C^w_{\mathrm{sc-CO_2}}$. The calculation for M_3 is as follows:

$$M_3 = S_{wr(\mathrm{sc-CO_2(max)})} \rho_{\mathrm{sc-CO_2}} C^w_{\mathrm{sc-CO_2}} V_p \tag{4}$$

where $C^w_{\mathrm{sc-CO_2}}$ denotes the dissolution coefficient of sc-CO_2 in the water phase (dissolution trapping), equal to 0.06 in this study (Zhang et al., 2010).

It should be noted that residual oil and water saturations can be measured through water flooding, the sc-CO_2 miscible injection process, or the Dean-Stark experiment when the core flooding experiments are completed (Zhou et al., 2023).

Once the recoverable oil has been recovered during the second sc-CO_2 miscible injection, the experimental composite core can be called a depleted core. Three phases exist within the core's pore space: maximum sc-CO_2 saturation, residual oil saturation, and residual water saturation. These factors are

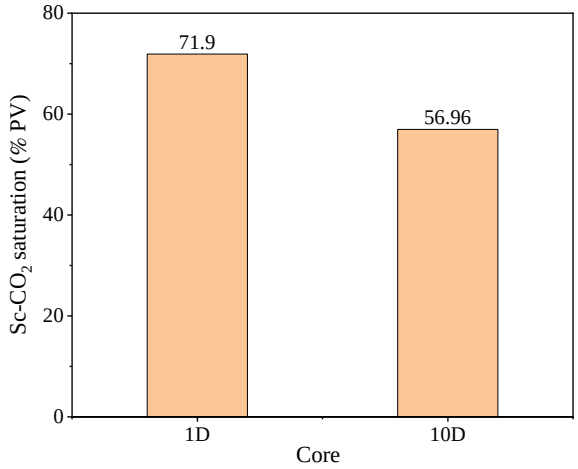

Fig. 2. Maximum sc-CO_2 saturation for composite cores 1D and 10D at the end of core flooding experiments.

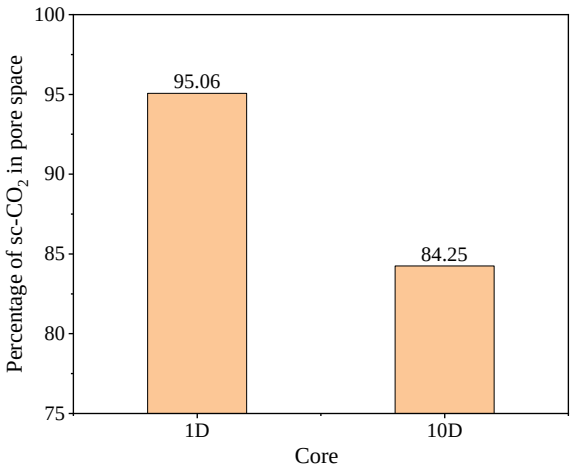

Fig. 4. Percentage of sc-CO_2 saturation in the pore space for composite cores 1D and 10D at the end of core flooding experiments.

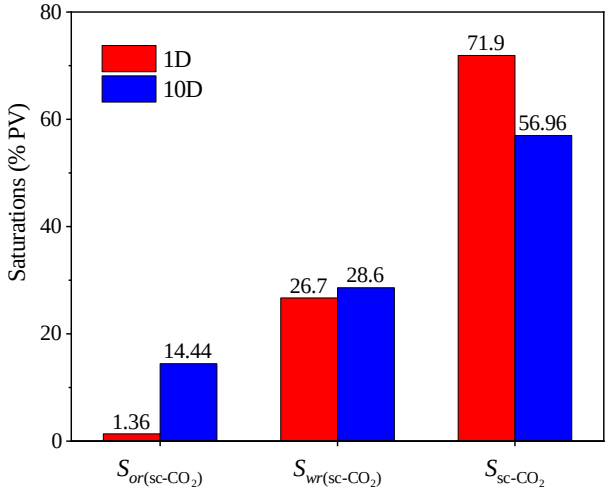

Fig. 3. Distribution of sc-CO_2 saturation and residual saturations for composite cores 1D and 10D at the end of core flooding experiments.

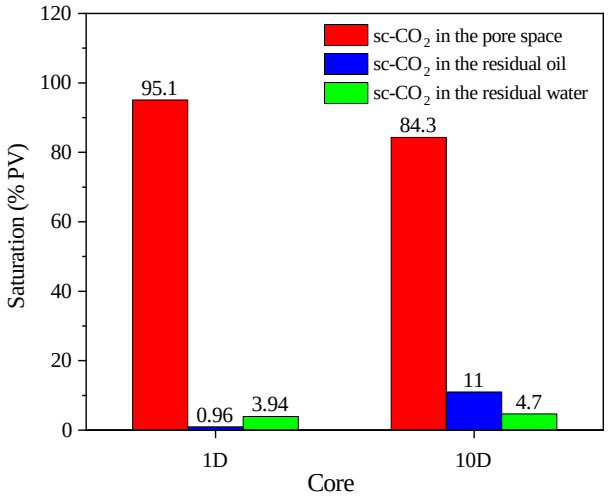

Fig. 5. Distribution of sc-CO_2 in the void space and residual phase saturation for composite cores 1D and 10D at the end of the core flooding experiments.

crucial in influencing geological sequestration in depleted oil reservoirs.

Maximum sc-CO_2 saturation: When evaluating the storage capacity of supercritical carbon dioxide in a depleted core based on laboratory experiment data, one crucial parameter is maximum sc-CO_2 saturation, which represents the extent of pore space occupied by the sc-CO_2 injection process. Figs. 2 and 3 illustrate the maximum sc-CO_2 saturation values and the distribution of sc-CO_2 and residual phases in the pore space after the sc-CO_2 miscible injection process, respectively.

The results indicate that the high permeable zone (HPCP) has a larger pore space available for sc-CO_2 storage compared to the low permeable zone (LPCP), as shown in Fig. 2. Fig. 4 demonstrates the sc-CO_2 percentage of the total pore space, while Fig. 5 presents the proportion of each phase in the pore space. According to the results in Fig. 4, the utilization efficiency of sc-CO_2 storage in the HPCP (95%) is much better than that of the LPCP (84%). The findings from Figs. 2 and 3 emphasize the significance of sc-CO_2 displacement efficiency, wherein higher efficiency in the core or field corresponds to greater storage capacity.

Residual saturation: In the depleted carbonate oil reservoir flooded by the sc-CO_2 miscible injection process at the last stage, aside from sc-CO_2, residual oil, and residual water are also present. A reliable experimental method has been proposed by Zhou et al. (2023) to quantify the values of these residual phases accurately. This method determines the oil and water content in the core plug during the first and second sc-CO_2 miscible injection. Fig. 6 displays the saturation distribution of sc-CO_2, residual oil, and water in composite cores 1D and 10D at the end of the sc-CO_2 miscible injection process. The dissolution trappings of sc-CO_2 in the residual oil and water depend on those saturations. Additionally, Fig. 3 compares the distribution of sc-CO_2 and residual phase saturations in the same composite cores, 1D and 10D. Table 7 presents a comprehensive list of these saturation values.

Table 7. Calculation of Sc-CO_2 storage capacity in core-scale.

Core	$S_{sc-CO_2(max)}$ (% PV)	M_1 (g)	$S_{orsc-CO_2}$ (% PV)	M_2 (g)	S_{wr} (% PV)	M_3 (g)	M_T (g)
1D	71.9	7.89	1.36	0.08	26.7	0.33	8.3
10D	56.96	4.28	14.44	0.56	28.6	0.24	5.1

Notes: M_T: Total sc-CO_2 storage capacity in the core; S_{or}: Residual oil saturation.

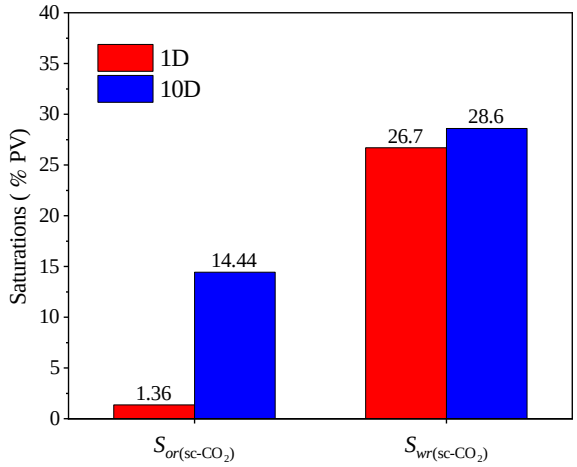

Fig. 6. Distribution of residual oil and water saturation for composite cores 1D and 10D at the end of the core flooding experiments.

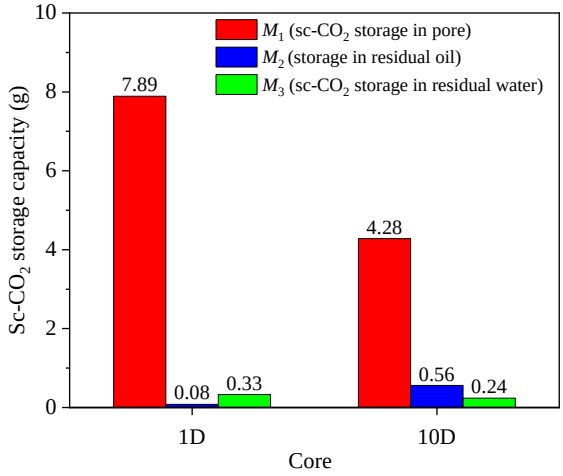

Fig. 7. Sc-CO_2 sequestration capacity in the pore space and residual phases for composite cores 1D and 10D at the end of the core flooding experiments.

Determination of Residual phase saturation: The pore space of the formation in the depleted oil reservoir contains two residual phases after the end of the sc-CO_2 miscible injection process: Residual oil and residual water. Both residual oil saturation and residual water saturation are involved in Eqs. (3) and (4). To determine the oil recovery factor and $S_{or(sc-CO_2)}$ (residual oil saturation), oil production is recorded during the first and second sc-CO_2 miscible injections, while water production is typically disregarded. However, Eq. (4) highlights the importance of considering the sc-CO_2 storage capacity, M_3, which results from the dissolution of sc-CO_2 in the residual water. In a previous study (Zhou et al., 2023), two methods were proposed to measure residual water saturation: The flooding experiment method and the Dean-Stark method. These methods aim to assess the sc-CO_2 storage capacity, considering both residual oil and water in the core. Table 7 presents the sc-CO_2 storage capacity caused by residual oil and water, which depends on the saturations of residual oil and water.

Evaluation of sc-CO_2 sequestration capacity in core-scale: considering the values of sc-CO_2 saturation, residual oil saturation, and residual water saturation provided in Table 7, Eqs. (2), (3), and (4) were utilized to calculate the sc-CO_2 storage capacity for each phase in grams. These sequestration capacity values are also listed in Table 7. Fig. 7 illustrates the proportion of sc-CO_2 sequestration capacity in the rock's pore, residual oil, and residual water for each phase. The findings indicate that the sc-CO_2 sequestration capacity in the pore space of the high permeable zone (composite core 1D) is higher compared to the low permeable zone (composite core 10D). This can be due to the influence of the maximum sc-CO_2 saturation, which depends on the displacement efficiency of the sc-CO_2 miscible injection process. The storage capacity restored by the pore structure or the maximum sc-CO_2 saturation is approximately 95.1% for the zone of high permeability (HPCP) and 84.3% for low permeability (LPCP). Reservoir heterogeneity or permeability contrast is another significant factor. The study demonstrates that reservoir heterogeneity impacts oil recovery through water flooding and sc-CO_2 miscible injection and influences sc-CO_2 storage potential in depleted oil reservoirs. The sc-CO_2 storage capacity in the HPCP are 8.3 and 5.1 g for LPCP, respectively, which is related to core properties and displacement efficiency of seawater flooding and sc-CO_2 miscible injection processes.

Improvement of sc-CO_2 sequestration capacity: During the first sc-CO_2 miscible injection, a significant portion of sc-CO_2 bypassed through the high permeable zone (composite core: 1D), resulting in around 30% of the pore volume of crude oil remaining in the low permeable zone (composite core: 10D). To improve displacement efficiency and sc-CO_2 storage capacity in the LPCP, a TFGS system was introduced into composite core 1D (HPCP) to block the high permeable zone. Fig. 8 demonstrates that approximately 41% of the pore volume was available for sc-CO_2 restoration after the first sc-CO_2 miscible injection, and an additional 15.6% of the pore volume was improved to restore sc-CO_2 capacity after the second sc-CO_2 miscible injection. This improvement was achieved by implementing the TFGS system in the high permeable composite core 1D. Experimental results confirm

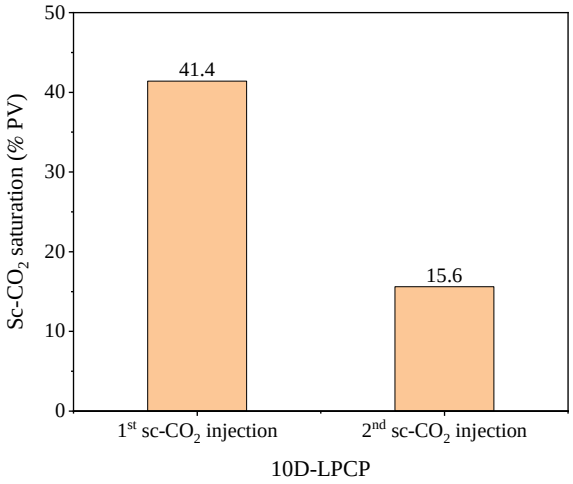

Fig. 8. Improvement of sc-CO_2 storage capacity in the low permeable zone (10D-LPCP) after injecting TFGS system into composite core 1D.

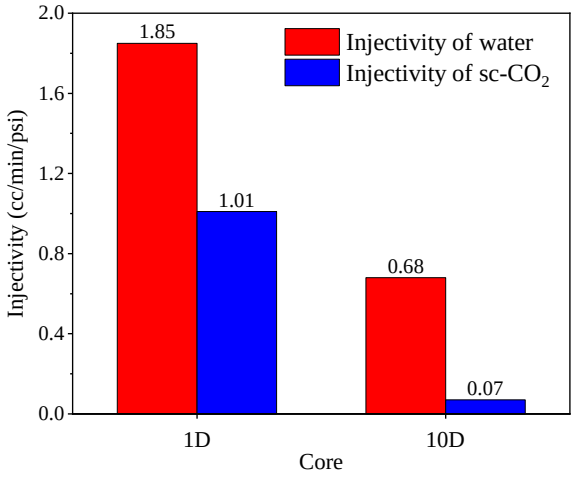

Fig. 9. Comparison of the injectivity of seawater flooding and second sc-CO_2 miscible injection.

that the injection of the TFGS system is a highly effective approach to enhancing sc-CO_2 storage capacity.

3.3 Dynamic characteristics parameter

In the study focused on sc-CO_2 sequestration in a depleted carbonate oil reservoir, two significant dynamic characteristics parameters were considered: injectivity and permeability loss. These parameters play an important role in determining the effectiveness of sc-CO_2 injection. Data from both water flooding and sc-CO_2 miscible injection were utilized to evaluate the injectivity and permeability loss. By analyzing these data, we can assess the effect of these parameters on the ability of sc-CO_2 injection for storage purposes.

3.3.1 Injectivity of sc-CO_2 miscible injection

Injectivity refers to the assessment of injection rate and pressure during the injection of treatment fluids into a targeted formation. These treatment fluids can include water, gas-CO_2, liquid-CO_2, sc-CO_2, polymer, and surfactant solutions, as documented in studies by Han et al. (2012) and Zhou et al. (2020b). In this work, seawater and sc-CO_2 were employed as displacing agents to conduct oil recovery experiments and evaluate the potential for sc-CO_2 storage. The expressions for the evaluation are as follows:

$$I_w = \frac{Q_w}{\Delta P_w} \tag{5}$$

and

$$I_{\mathrm{sc-CO_2}} = \frac{Q_{\mathrm{sc-CO_2}}}{\Delta P_{\mathrm{sc-CO_2}}} \tag{6}$$

where I_w and $I_{\mathrm{sc-CO_2}}$ represent the injectivity of seawater flooding for the secondary oil recovery and sc-CO_2 miscible injection process for tertiary oil recovery, respectively; Q_w and $Q_{\mathrm{sc-CO_2}}$ denote the injection flow rate during seawater and sc-CO_2 injection process; ΔP_w and $\Delta P_{\mathrm{sc-CO_2}}$ represent the differential pressure across the core sample, respectively. The parameters in Eqs. (5) and (6) can be measured during the seawater and sc-CO_2 miscible injection process.

Several parameters affect the injectivity of CO_2 injection in depleted oil reservoirs, such as mineral grain falloff, fine particle migration, and residual phases. Fig. 9 compares injectivities between seawater flooding and sc-CO_2 miscible injection cases. It is crucial to note that injectivity is calculated using stable differential pressure data before the experiment of sc-CO_2 miscible injection is terminated. The experimental results indicate a decrease in injectivity for both composite cores, 1D and 10D. Specifically, for composite core 1D, injectivity declines from 1.85 to 1.01, and for composite core 10D, it reduces from 0.68 to 0.07. The observed decrease in injectivity suggests varying degrees of core sample damage, likely attributed to a combination of mineral grain falloff, fine particle migration, which can block the pore throat of the pore system, and interactions within the seawater/sc-CO_2/carbonate rock system (Sokama-Neuyam et al., 2017, Yusof et al., 2022). For the depleted oil reservoirs, the influence of the residual phases on injectivity can not be ignored in this study. The experimental results highlight that the high permeable core (HPCP) experienced more damage than the low permeable core (LPCP). The HPCP has an initial permeability of 832 mD, while the LPCP has 69 mD. The injectivity of the high permeable core, 1D, is reduced by approximately 54% based on the brine permeability after the end of sc-CO_2 miscible injection, primarily due to mineral grain falloff and fine particle migration. However, for the case of the low permeable core, 10D, injectivity is reduced relatively small, about 10%. This phenomenon may be related to the compaction degree of the formation.

3.3.2 Permeability loss and endpoint relative permeability

The sc-CO_2 miscible injection involves a two-phase flow: the water phase and the miscible phase consisting of sc-CO_2 and crude oil. Zhou et al. (2019) reported the two-phase relative permeability of the seawater and miscible phases. In this study, our main focus is investigating the permeability loss and relative permeability at the endpoints resulting from the sc-CO_2 miscible injection.

The evaluation of permeability loss is based on the initial

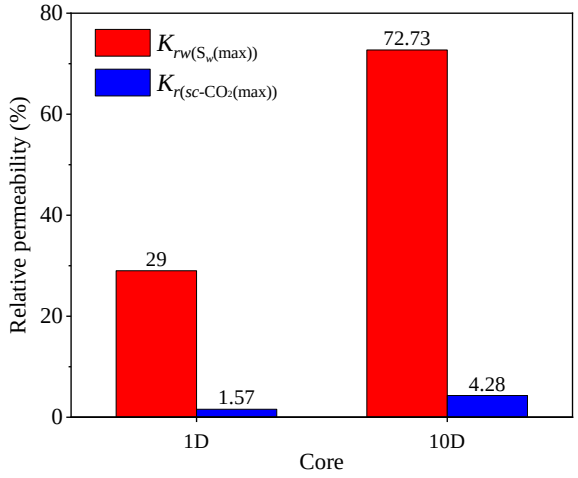

Fig. 10. Comparison of the endpoint relative permeabilities of 1D and 10D during seawater flooding and second sc-CO_2 miscible injection process.

brine permeability before any fluid injection process. Table 3 lists the brine permeabilities for composite cores 1D and 10D, with values of 750 and 22.3 mD, respectively.

For composite core 1D, after the completion of seawater flooding, the permeability decreased from 750 to 218 mD at a remaining oil saturation of about 37% of the pore volume, resulting in a permeability loss of approximately 532 mD. The endpoint relative permeability for the seawater phase was about 29% at the remaining oil saturation. In other words, after the sc-CO_2 miscible injection, the sc-CO_2 permeability was 11.78 mD, with a relative permeability of approximately 1.6%. This indicates a permeability loss of about 27% compared to the endpoint relative permeability of seawater flooding. Fig. 10 illustrates these values. For the LPCP (10D), the permeability after seawater flooding reduced to about 6.1 mD from the initial value of 22.3 mD (see Table 3). Based on the brine permeability, the seawater relative permeability at the remaining oil saturation was approximately 73%. At the end of the sc-CO_2 miscible injection, the sc-CO_2 permeability was 0.95 mD, with a relative permeability to sc-CO_2 of about 4.28%.

Fig. 10 shows that the relative permeability of both LPCP (10D) and HPCP (1D) decreases to varying degrees during seawater flooding and the sc-CO_2 miscible injection process. This observation suggests that the residual oil saturation also influences the decrease of absolute and relative permeability and the interaction between sc-CO_2/seawater and carbonate rock.

Despite the decrease in both injectivity and relative permeability at the end of sc-CO_2 miscible injection, these factors do not significantly impact the injection process for geologic sequestration of sc-CO_2 in depleted oil reservoirs because the injection pressure caused by sc-CO_2 injection reached a constant value.

4. Conclusions

The conclusions drawn from the dual-core flooding experiments, which encompassed seawater flooding, initial sc-CO_2 miscible injection, thermal foam gel slug system, and second sc-CO_2 miscible injection at reservoir conditions, are as follows:

1) Reservoir heterogeneity significantly impacts secondary oil recoveries through seawater flooding, tertiary oil recovery through sc-CO_2 miscible injection, and the sc-CO_2 storage capacity in the low permeable formation.
2) The method of injecting the thermal foam gel slug system into the high permeable zone proposed in this study not only enhances displacement efficiency but also increases the storage capacity of sc-CO_2 in the low permeable zone, which is about 15% of the pore volume.
3) Despite the observed decrease in injectivity and permeability during sc-CO_2 injection compared to seawater flooding, it does not hinder the injection process for sc-CO_2 geological storage based on the endpoint relative permeability of sc-CO_2.
4) Assessment of sc-CO_2 storage capacity in depleted carbonate oil reservoirs has been conducted at the core scale, with structural trapping identified as a pivotal mechanism for these reservoirs.
5) The sc-CO_2 storage potential is directly linked to reservoir properties, particularly permeability, with higher permeability translating to greater sc-CO_2 storage capacity.

By conducting these experimental investigations, this study contributes to understanding the effect of reservoir heterogeneity on sc-CO_2-EOR and its sequestration in depleted carbonate oil reservoirs. The findings will provide insights into the design and optimization of injection strategies, conformance control techniques, and reservoir management practices to maximize the efficiency and effectiveness of sc-CO_2-EOR and sequestration.

Acknowledgements

The researchers express their gratitude to the Center for Integrative Petroleum Research (CIPR), College of Petroleum & Geosciences (CPG), and King Fahd University of Petroleum & Minerals (KFUPM) for their support and publication of this study.

Additional information: Author's email

ywu@mines.edu (Y. -S. Wu).

Conflict of interest

The authors declare no competing interest.

References

Al-Bayati, D., Saeedi, A., Xie, Q., et al. Influence of permeability heterogeneity on miscible CO_2 flooding efficiency in sandstone reservoirs: An experimental investigation. Transport in Porous Media, 2018, 125: 341-356.

Alfarge, D., Wei, M., Bai, B. Factors affecting CO_2-EOR in

shale-oil reservoirs: Numerical simulation study and pilot tests. Energy & Fuels, 2017, 31(8): 8462-8480.

AlOtaibi, F. M., Zhou, X., Abdulla Habah, A., et al. EOR by CO_2 emulsions better sweep efficiency and improved recovery. Paper SPE 183014 Presented at the Abu Dhabi International Petroleum Exhibition & Conference, Abu Dhabi, UAE, 7-10 November, 2016.

Al-Otaibi, F. M., Zhou, X., Kokal, S. L. Laboratory evaluation of different modes of supercritical carbon dioxide miscible flooding for carbonate rocks. SPE Reservoir Evaluation & Engineering, 2018, 22(1): 137-149.

AlRassas, A. M., Ren, S., Sun, R., et al. CO_2 storage capacity estimation under geological uncertainty using 3-D geological modeling of unconventional reservoir rocks in Shahejie Formation, block Nv32, China. Journal of Petroleum Exploration and Production Technology, 2021, 11(6): 2327-2345.

Ampomah, W., Balch, R. S., Grigg, R. B., et al. Co-optimization of CO_2-EOR and storage processes in mature oil reservoirs. Greenhouse Gases: Science and Technology, 2017, 7(1): 128-142.

Bachu, S. Sequestration of CO_2 in geological media: Criteria and approach for site selection in response to climate change. Energy Conversion and Management, 2000, 41(9): 953-970.

Benson, S. M., Bennaceur, K., Cook, P., et al. Carbon capture and storage, in Global Energy Assessment-Toward a Sustainable Future, edited by T. B. Johansson, A. Patwardhan, N. Nakicenovic and L. Gomez-Echeverri, Cambridge University Press, Cambridge, pp. 993-1068, 2012.

Cao, C., Liu, H., Hou, Z., et al. A review of CO_2 storage in view of safety and cost-effectiveness. Energies, 2020, 13(3): 600.

Carroll, A. G., Przeslawski, R., Radke, L., et al. Environmental considerations for subseabed geological storage of CO_2: A review. Continental Shelf Research, 2014, 83: 116-128.

Ding, M., Yuan, F., Wang, Y., et al. Oil recovery from a CO_2 injection in heterogeneous reservoirs: The influence of permeability heterogeneity, CO_2-oil miscibility, and injection pattern. Journal of Natural Gas Science and Engineering, 2017, 44: 140-149.

Ding, S., Liu, G., Li, P., et al. CO_2 storage capacity estimation in tertiary and depleted oil reservoirs. Paper IPTC 19219 Presented at International Petroleum Technology Conference, Beijing, China, 26-28 March, 2019.

Ding, S., Wen, F., Wang, N., et al. Multi-objective optimization of CO_2 enhanced oil recovery and storage processes in low permeability reservoirs. International Journal of Greenhouse Gas Control, 2022, 121: 103802.

Enick, R. M., Olsen, D. K., Ammer, J. R., et al. Mobility and conformance control for CO_2 EOR via thickeners, foams, and gels-a literature review of 40 years of research and pilot tests. Paper SPE 154122 Presented at the SPE Improved Oil Recovery Symposium, Tulsa, Oklahoma, 14-18 April, 2012.

Ennis-King, J., Paterson, L. Engineering aspects of geological sequestration of carbon dioxide. Paper SPE 77809 Presented at the SPE Asia Pacific Oil and Gas Conference and Exhibition, Melbourne, Australia, 8-10 October, 2002.

Ettehadtavakkol, A., Lake, L.W., Bryant, S. L. CO_2-EOR and storage design optimization. International Journal of Greenhouse Gas Control, 2014, 25: 79-92.

Fernø, M., Steinsbø, M., Eide, Ø., et al. Parametric study of oil recovery during CO_2 injections in fractured chalk: Influence of fracture permeability, diffusion length, and water saturation. Journal of Natural Gas Science and Engineering, 2015, 27: 1063-1073.

Hadipoor, M., Taghavi, H., Taghavi, H. Experimental investigation of CO_2 injection performance in heterogeneous reservoirs: Parametric analysis. Petroleum Science and Technology, 2020, 38: 837-848.

Han, M., Zhou, X., Alhasan, F. B., et al. Laboratory investigation of the injectivity of sulfonated polymer solutions into carbonate reservoir rocks. Paper SPE 155390 Presented at the SPE EOR Conference at Oil and Gas West Asia, Muscat, Oman, 16-18 April, 2012.

Hannis, S., Lu, J., Chadwick, A., et al. CO_2 storage in depleted or depleting oil and gas fields: What can we learn from existing projects? Energy Procedia, 2017, 114: 5680-5690.

Imanovs, E., Krevor, S., Zadeh, A. M. CO_2-EOR and storage potentials in depleted reservoirs in the Norwegian continental shelf NCS. Paper SPE 200560 Presented at the SPE Europec, Virtual, 1-3 December, 2020.

International Energy Agency (IEA). Whatever happened to enhanced oil recovery? International Energy Agency, 2018.

International Energy Agency (IEA). Updates EOR project data, doubling output forecast. Oil & Gas Journal, 2019.

Kalra, S., Tian, W., Wu, X. A numerical simulation study of CO_2 injection for enhancing hydrocarbon recovery and sequestration in liquid-rich shales. Petroleum Science, 2018, 15: 103-115.

Khosravi, M., Bahramian, A., Emadi, M., et al. Mechanistic investigation of bypassed oil recovery during CO_2 injection in matrix and fracture. Fuel, 2014, 117: 43-49.

Kokal, S., Al-Kaabi, A. Enhanced oil recovery: Challenges & opportunities. World Petroleum Council: Technology and Innovation, Global Energy Solutions, 2010, 64(1): 64-69.

Korbøl, R., Kaddour, A. Sleipner vest CO_2 disposal-injection of removed CO_2 into the utsira formation. Energy Conversion and Management, 1995, 36: 509-612.

Li, Z., Gu, Y. Soaking effect on miscible CO_2 flooding in a tight sandstone formation. Fuel, 2014, 134: 659-668.

Luo, J., Hou, Z., Feng, G., et al. Effect of reservoir heterogeneity on CO_2 flooding in tight oil reservoirs. Energies, 2022, 15(9): 3015.

Okasha, T. M., Funk, J. J., Al-Rashid, H. N. Fifty years of wettability measurements in the Arab-D carbonate reservoir. Paper SPE 105114 Presented at the SPE Middle East Oil and Gas Show and Conference, Manama, Bahrain, 11-14 March, 2007.

Orlic, B. Geomechanical effects of CO_2 storage in depleted gas reservoirs in the Netherlands: Inferences from feasi-

bility studies and comparison with aquifer storage. Journal of Rock Mechanics and Geotechnical Engineering, 2016, 8(6): 846-859.

Sæle, A., Graue, A., Alcorn, Z. P. Unsteady-state CO_2 foam injection for increasing enhanced oil recovery and carbon storage potential. Advances in Geo-Energy Research, 2022, 6(6): 472-481.

Sengul, M. CO_2 sequestration - A safe transition technology. Paper SPE 98617 Presented at the SPE International Health, Safety & Environment Conference, Abu Dhabi, UAE, 2-4 April, 2006.

Shaw, J., Bachu, S. Screening, evaluation, and ranking of oil reservoirs suitable for CO_2 flood EOR and carbon dioxide sequestration. Journal of Canadian Petroleum Technology, 2002, 41(9): 51-61.

Shen, P., Liao, X., Liu, Q. Methodology for estimation of CO_2 storage capacity in reservoirs. Petroleum Exploration and Development, 2009, 36(2): 216-220.

Sokama-Neuyam, Y. A., Forsetløkken, S. L., Lien, J., et al. The coupled effect of fines mobilization and salt precipitation on CO_2 injectivity. Energies, 2017, 10(8): 1125.

Steinsbø, M., Brattekas, B., Fernø, M. A., et al. Supercritical CO_2 injection for enhanced oil recovery in fractured chalk. Paper SCA2014-092 Presented at International Symposium of the Society of Core Analysts, Avignon, France, 8-11 September, 2014.

Sun, L., Chen, W. Assessment of CO_2 geo-storage potential in an onshore oil reservoir, China. China Population, Resources, and Environment, 2012, 22(6): 76-81. (in Chinese)

Wei, B., Wang, B., Li, X., et al. CO_2 storage in depleted oil and gas reservoirs: A review. Advances in Geo-Energy Research, 2023, 9(2): 76-93.

Yue, P., Zhang, R., Sheng, J. J., et al. Study on the influential factors of CO_2 storage in low permeability reservoir. Energies, 2022, 15(1): 344.

Yusof, M. A. M., Neuyam, Y. A. S., Ibrahim, M. A., et al. Experimental study of CO_2 injectivity impairment in sandstone due to salt precipitation and fines migration. Journal of Petroleum Exploration and Production Technology, 2022, 12: 2191-2202.

Zhang, L., Chen, L., Hu, R., et al. Subsurface multiphase reactive flow in geologic CO_2 storage: Key impact factors and characterization approaches. Advances in Geo-Energy Research, 2022, 6(3): 179-180.

Zhang, L., Nowak, W., Oladyshkin, S., et al. Opportunities and challenges in CO_2 geologic utilization and storage. Advances in Geo-Energy Research, 2023, 8(3): 141-145.

Zhang, Y., Zhang, L., Niu, B., et al. Integrated assessment of CO_2-enhanced oil recovery and storage capacity. Paper SPE 137615 Presented at the Canadian Unconventional Resources and International Petroleum Conference, Calgary, Alberta, Canada, 19-21 October, 2010.

Zhou, X., Al-Otaibi, F., Kokal, S. Relative permeability characteristics and wetting behavior of supercritical CO_2 displacing water and remaining oil for carbonate rocks at reservoir conditions. Energy & Fuels, 2019, 33(6): 5464-5475.

Zhou, X., AlOtaibi, F. M., Kamal, M. S., et al. Effect of conformance control patterns and size of the slug of In Situ supercritical CO_2 emulsion on tertiary oil recovery by supercritical CO_2 miscible injection for carbonate reservoirs. ACS Omega, 2020a, 5(51): 33395-33405.

Zhou, X., Kamal, M. S., Fuseni, A. B. Comprehensive investigation of dynamic characteristics of amphoteric surfactant-sulfonated polymer solution on carbonate rocks in reservoir conditions. ACS Omega, 2020b, 5(29): 18123-18133.

Zhou, X., Yu, W., Wu, Y., et al. Dynamic characteristics of supercritical CO_2 injection in depleted carbonate oil reservoir for its sequestration potential: An experimental study. Paper SPE 213591 Presented at the Middle East Oil, Gas and Geosciences Show, Manama, Bahrain, 19-21 February, 2023.